A 3D wave model to simulate the interaction of wave field in the presence of multi-structures

Zaman, M. Hasanat; Winsor, Fraser

Publisher's version / Version de l'éditeur:
http://doi.org/10.1109/OCEANS.2014.7003299
2014 Oceans - St. John's, OCEANS 2014, 2014-09-14

A 3D wave model to simulate the interaction of wave field in the presence of multi-structures

M. Hasanat Zaman and Fraser Winsor

Ocean, Coastal and River Engineering
National Research Council Canada
Arctic Avenue P.O.Box 12093
St. John's NL A1B 3T5
Emails: Hasanat.Zaman@nrc-cnrc.gc.ca; Fraser.Winsor@nrc-cnrc.gc.ca

Abstract

A 3D dispersive numerical model has been developed and utilized to study the interacted wave field in the Offshore Engineering Basin (OEB) of National Research Council Canada in the presence of array of structures. The basic physics of the numerical model follows the concept of the depth averaged velocity distribution along with an enhanced dispersion relation. The Alternating Direction Implicit (ADI) algorithm has been employed for the solution of the governing equations. As an application, the model has been used to study the wave propagation in the presence of different combinations of structures where the effects due to the reflection and diffraction are also incorporated. Relevant experiments are carried out in the OEB. Total 10 wave probes are deployed to measure the data at different locations in the Basin. Later the numerical results are compared with the experimental results in the OEB at different probe locations for different wave and structure conditions. The comparisons of the numerical results show great agreement with the experimental results. In this paper the results for regular waves will only be presented and discussed.

Introduction

The deployment locations of the structures that capture waves' energies significantly depend on the magnitude of the incoming wave fields and their directions. In addition to that the location of each structure in the array has to be well located such that each of them can see almost the similar incoming wave field. This is a very important requirement for the farm array establishment. The present work is to study the propagation, reflection and diffraction of an incoming wave field in the presence of structures assumed to be the wave energy extracting device in different arrays. This study will give an insight for better array setup in order to capture wave energy from a given wave field. The purpose of the present work is to compare the numerical results with the relevant experimental results that obtained from the experiment in the OEB at different locations.

Governing Equations

The basic continuity equation and the equations of motion involved in this model can be described in the following way:

$$\eta_t + P_x + Q_y = 0 \tag{1}$$

$$P_t + \left(P^2/D\right)_x + \left(PQ/D\right)_y + gD\eta_x + \varepsilon P + \frac{f}{2D^2} P\sqrt{P^2+Q^2} = \nu\left(P_{xx} + P_{yy}\right) + \left(B + \frac{1}{3}\right)h^2\left(P_{xxt} + Q_{xyt}\right) + Bah^3\left(\eta_{xxx} + \eta_{xyy}\right) + hh_x\left(\frac{1}{3}P_{xt} + \frac{1}{6}Q_{yt}\right) + hh_y\left(\frac{1}{6}Q_{yt}\right) + Bgh^2\left[h_x\left(2\eta_{xx} + \eta_{yy}\right) + h_y\eta_{xy}\right] \tag{2}$$

$$Q_t + \left(PQ/D\right)_x + \left(Q^2/D\right)_y + gD\eta_y + \varepsilon Q + \frac{f}{2D^2} Q\sqrt{P^2+Q^2} = \nu\left(Q_{xx} + Q_{yy}\right) + \left(B + \frac{1}{3}\right)h^2\left(Q_{yyt} + P_{xyt}\right) + Bah^3\left(\eta_{yyy} + \eta_{xxy}\right) + hh_y\left(\frac{1}{3}Q_{yt} + \frac{1}{6}P_{xt}\right) + hh_x\left(\frac{1}{6}P_{yt}\right) + Bgh^2\left[h_y\left(2\eta_{yy} + \eta_{xx}\right) + h_x\eta_{xy}\right] \tag{3}$$

where η is the instantaneous water surface elevation, P the depth integrated velocity component (flux) in the x-direction, Q the depth integrated velocity component (flux) in the y-direction, h the local still water depth, D (=h+η) the local instantaneous water depth, g the gravitational acceleration, ε the boundary dumping function varies linearly along the width of the sponge layers and null elsewhere, ν the eddy viscosity describes the momentum exchange due to turbulence, f the energy dissipation coefficient and the subscripts x, y and t denote the differentiation with respect to space and time. The parameter B is an important factor in the dispersion relation that depreciates the computational error in the wave celerity and group velocity.

The expression for ν can be given in the following way (Sato et al., 1992 and Bayram and Larson, 2000):

$$\nu = \frac{\alpha_D gd\tan\delta}{\sigma^2}\sqrt{\frac{g}{d}\frac{\hat{Q} - Q_r}{Q_s - Q_r}} \tag{4}$$

in which α_D is a coefficient (2.5 in the surf zone and null elsewhere), $\tan\delta$ the bottom slope, d the mean water depth and σ is the angular frequency. $\hat{Q}$ is the flow amplitude, Q_s the wave induced flow inside the surf zone and Q_r is the flow amplitude of the reform waves and are expressed as follows:

$$Q_s = 0.4(0.57 + 5.3\tan\delta)\sqrt{gd^3} \tag{5}$$

$$Q_r = 0.135\sqrt{gd^3} \tag{6}$$

Energy dumping event in a sponge layer follows the following relation:

$$\varepsilon_j = \frac{\gamma\varepsilon_m}{2(\sinh\gamma - \gamma)}\left[\cosh(\gamma X_j / F) - 1\right] \quad ; \quad j = 1, 2 \tag{7}$$

where the term ε_j is the boundary damping function and is null elsewhere apart from the

boundary, $\varepsilon_m = \sqrt{gh}$, γ is a coefficient, F is the width of the sponge layer and X_j is the horizontal distance along the sponge layer in the x and y directions, respectively. In the numerical computation we have adopted γ = 1. In this computation sponge layer is introduced to eliminate or reduce any reflection from the beach.

The wave number would be evaluated from the following dispersion relation in which B is equal to 1/15 corresponds to the frequency dispersion obtained from Padé's (2,2) expansion of the Stoke's first-order theory.

$$\frac{c^2}{gh} = \frac{1 + Bk^2h^2}{1 + (B + \frac{1}{3})k^2h^2} \tag{8}$$

where k is the wave number and c is the wave celerity.

Numerical Model

A Finite difference numerical method was employed for the solution of the governing equations. The discretization of Eq.1 to Eq.3 was done following the mesh shown in Fig. 1. The above governing equations were discretized in such a way so that the solution could be obtained by ADI algorithm. The discretized equations are not shown here however, for details please refer to Zaman et al. (2000, 2001).

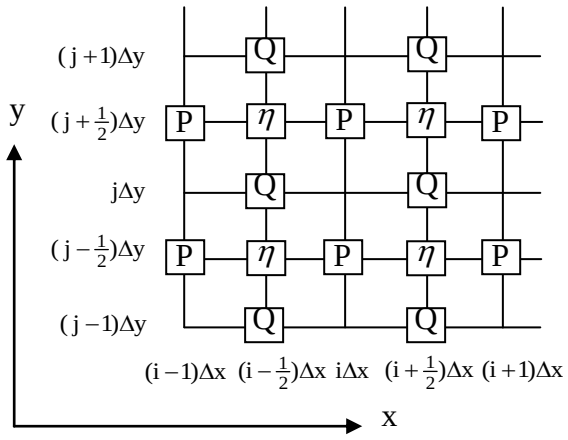

Fig. 1 Computational mesh

Description of the Experimental Setup

The experiment was carried out at the Offshore Engineering Basin of National Research Council Canada. The top view of the basin is shown in Fig. 2. The Offshore Engineering Basin is 75 m long x 32 m wide. 56 independently controlled segmented wave generators installed on the west wall generated the waves. Each segmented wave generator is 2 m high and 0.5 m wide. Passive absorbers, made of expanded metal sheets

with varying porosities and spacing, are installed on the east wall. A solid metal wall is used to cover the north side of the basin. The water depth for the experiments is 0.8m and 2.8m. However, the cases presented and discussed in this paper are confined to the 0.8m water depth experiments.

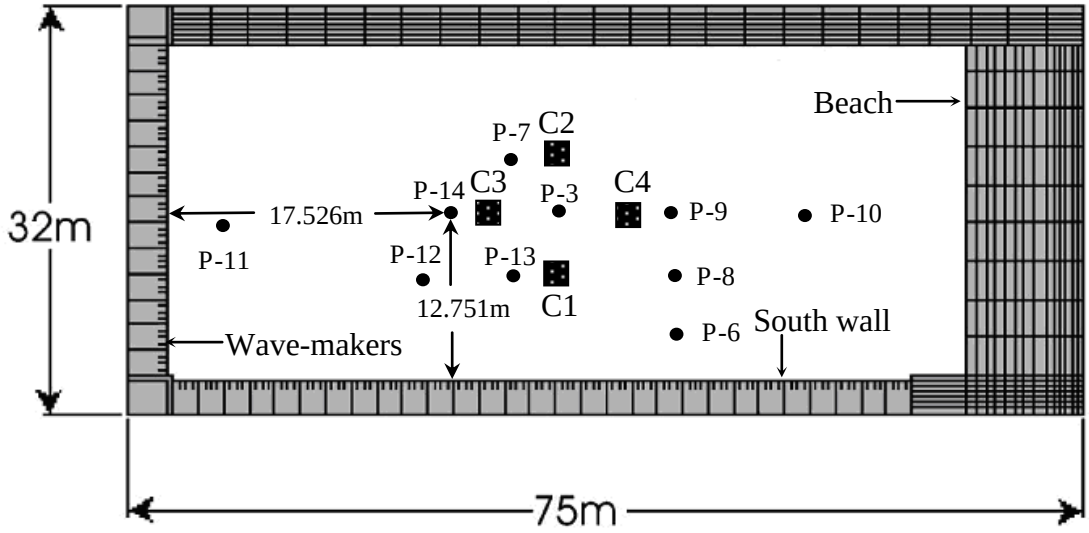

Fig. 2: Layout of the experimental tank (not to scale)

During the experiment, 10 wave probes were used as shown in Fig. 2 and Table 1 shows the location of the wave probes in the basin. All the wave probes are capacitance type. Table 2 shows the locations of the columns (C1-C2-C3-C4) in the basin. Each column is of square cross-section with 0.8m sides. All the data was acquired using GDAC (GEDAP Data Acquisition and Control) client-server acquisition system, developed by National Research Council Canada.

Table 1 Location of the wave probes in the OEB

No of the probe	Distance from the west wave paddle (m)	Distance from the south wall (m)
3	24.756	12.758
6	31.654	4.593
7	21.582	16.844
8	31.651	8.678
9	31.651	12.754
10	38.541	12.763
11	1.268	12.746
12	11.557	8.697
13	21.632	8.716
14	**17.526**	**12.751**

Table 2 Location of the Columns in the OEB

Columns	Distance from the east wave paddle (m)	Distance from the south wall (m)
Column 1 (C1)	24.697	8.672
Column 2 (C2)	24.715	16.803
Column 3 (C3)	20.619	12.762
Column 4 (C4)	28.766	12.742

Results and Discussions

In the present work regular waves over uniform water depth of 0.8m were used. Three different cases are chosen for the comparisons of the experimental data with the numerical results. Table 3 summarizes the incident wave parameters of the wave conditions examined in this report. In the table h is the still water depth, T is the wave period, H is the wave height, L is the wavelength, h/L is the relative water depth and H/L is the steepness of the incident waves.

Table 3 Incident wave parameters

	h (m)	T (s)	H (m)	h/L	H/L
Case-1	0.8	0.982	0.08	0.53	5%
Case-2	0.8	1.436	0.15	0.26	5%
Case-3	0.8	1.736	0.20	0.20	5%

Comparisons of Numerical and Experimental Results

Figs. 3, 4 and 5 respectively, show the comparisons of the numerical results with the experimental results of the surface elevations at probe locations P-14, P-3, P-9, P-12 and P-13 (Probes 14-3-9-13-14) for Case-1, Case-2 and Case-3 when the bottom is essentially flat and no column is in presence. It may be observed from the comparisons that in all three cases numerical results show good agreement with the experimental results for flat bottom.

For Case-3, Fig. 6 compares numerical results with the experiments when column 3 (C3) is in presence on the flat bottom of the basin. In the figure comparisons are shown at the locations of Probes 14-3-9-13-14. Again for Case-3, Fig. 7 shows similar comparisons at Probes 14-3-9-13-14 in the presence of columns 1 and 3 on the flat bottom. On the other hand, for Case-3, Fig. 8 also shows analogous comparisons at Probes 14-3-9-13-14 in the presence of columns 1, 2, 3 and 4.

In the presence of the structure(s) in the wave field, the flow condition becomes very complicated due to the inevitable reflected and diffracted waves. From the above results it may be observed that numerical results agree very well with the experimental results in the presence or in the absence of single or multiple structures in the wave field.

Numerical Results for Case-3

In the open sea the transmitted boundary is usually assumed to be an open boundary to make sure that transmitted, reflected and diffracted waves would not come back in the computational domain. To simulate the wave field within these criteria we have introduced energy damping layer or sponge layer (defined by Eq. 7) on the three sides of the computational domain as shown by red dotted lines in Fig. 9. This sponge layer is used to absorb all or most of the energy that penetrates into them and thus reduce reflections from the side walls or beach. We did not introduce any sponge layer over the incident boundary in order to account for the effects of the reflected wave components from the structure(s) on the incident waves. At least a two-wavelength (2L) width of the sponge layer is necessary to absorb most of the energy incident to them. A wider width of the sponge layer would provide much accuracy in the final results than any shorter width.

In this numerical computation, Case-3 has been utilized. Fig 9 shows the surface elevation normalized by the incident wave height on a flat bottom. On the other hand, Figs.10: (a), (b), (c) and (d) show the wave heights distribution normalized by the incident wave height for Column 3 (C3), Columns 1 & 2 (C1-C2), Columns 1 & 3 (C1-C3) and Columns 1, 2, 3 & 4 (C1-C2-C3-C4) respectively.

Conclusions

The model formulated and reported here is capable to study the wave propagation, reflection and diffraction problem in the presence of ocean structures in shallow to moderately deep water in 3D flow field. The model results show great agreement with relevant experimental results in the presence or in the absence of ocean structures. This model is capable to identify the high waves' zone where ocean energy extracted equipment can be installed for high performance.

References

Bayram, A. and M. Larson (2000): Wave transformation in the nearshore zone: comparison between a Boussinesq model and field data, Coastal Engineering, Elsevier, 39, pp.149-171.

Sato, S., M. Kabiling and H. Suzuki (1992): Prediction of near bottom velocity history by a non-linear dispersive wave model, Coastal Engineering in Japan 35(1), pp.68-82.

Zaman, M. H, Hirayama, K. and Hiraishi, T. (2001): An extended Boussinesq model and its application to long period waves. Proc. 11th Int. Offshore and Polar Eng. Conf., ISOPE-2001, Stavanger, Norway, Vol. III, pp.607-614.

Zaman, M. H, Hirayama, K. and Hiraishi, T. (2000): A Boussinesq Model to Study Long period waves in a harbor. Report of the Port and Harbor Research Institute, Japan. Vol.39, No.4, pp.25-50.

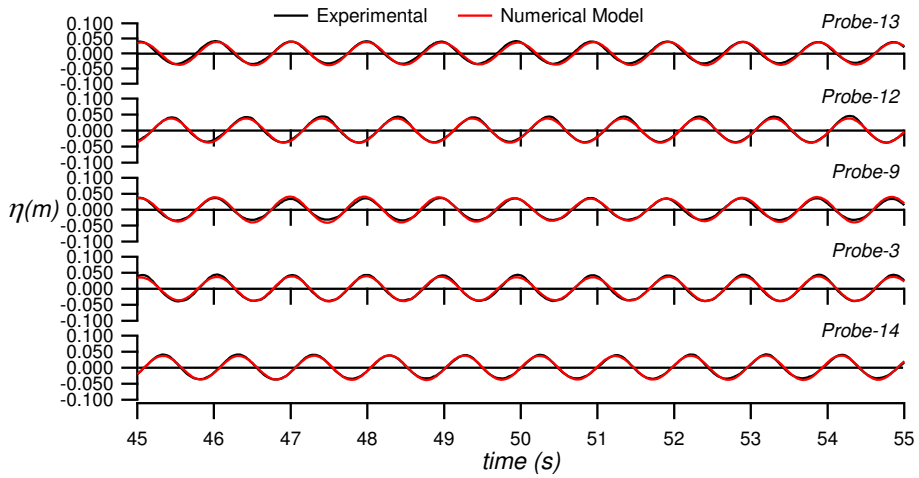

Fig. 3 Surface elevations at different probe locations in the absence of any structure (Case2: h=0.8m, H=0.08m, T=0.982s, h/L=53.2% and H/L=5%; No structure)

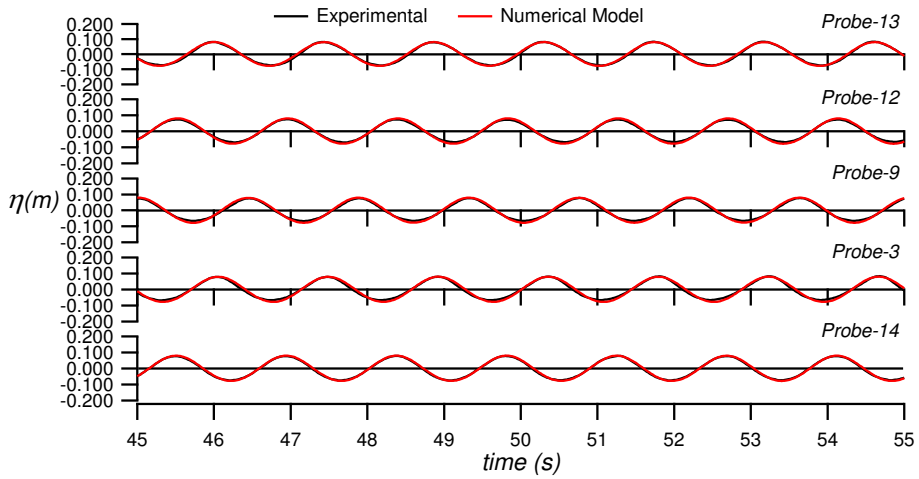

Fig. 4 Surface elevations at different probe locations in the absence of any structure (Case3: h=0.8m, H=0.15m, T=1.436s, h/L=26.7% and H/L=5%; No structure)

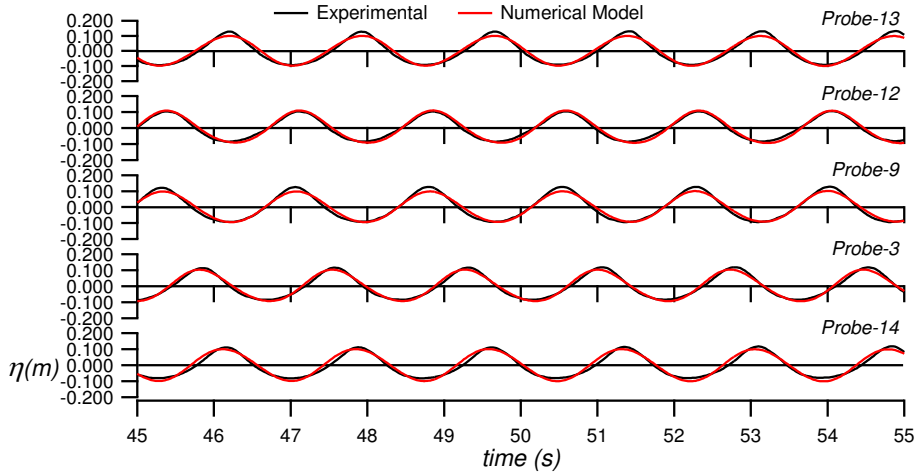

Fig. 5 Surface elevations at different probe locations in the absence of any structure (Case3: h=0.8m, H=0.20m, T=1.736s, h/L=20% and H/L=5%; No structure)

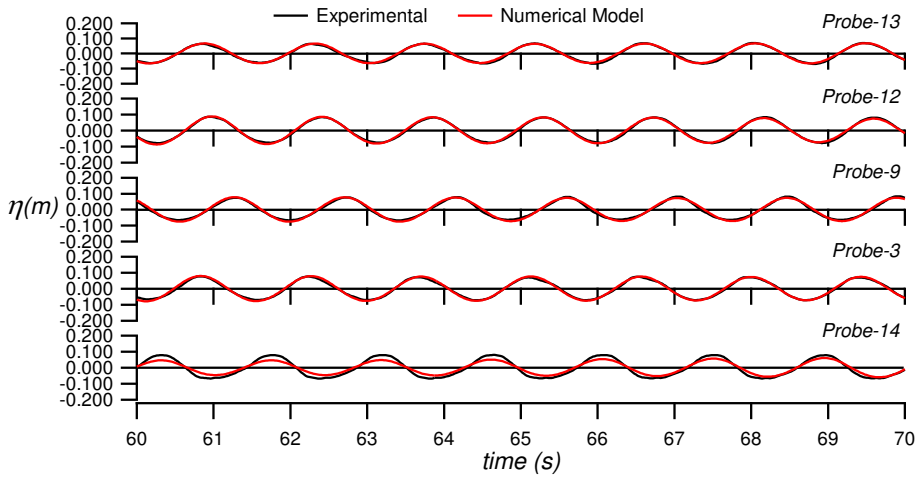

Fig. 6 Surface elevations at different probe locations in the presence of Column 3 (Case3: h=0.8m, H=0.15m, T=1.436s, h/L=26.7% and H/L=5%; C3)

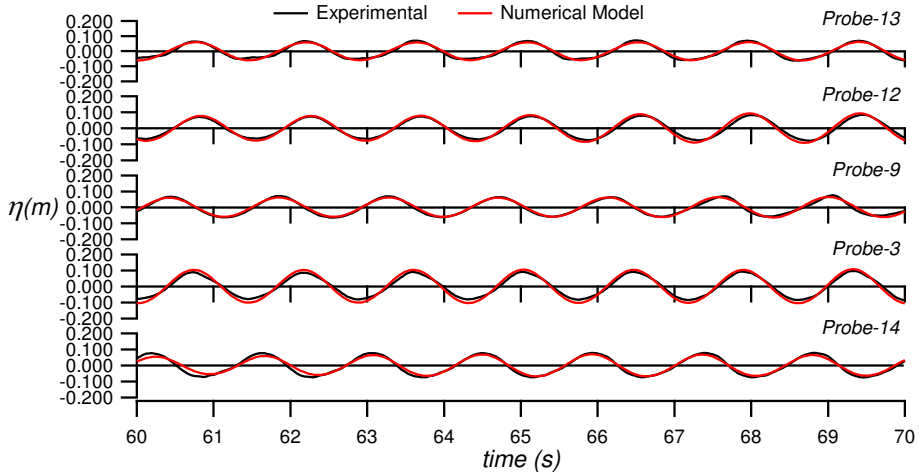

Fig. 7 Surface elevations at different probe locations in the presence of Columns 1-3 (Case3: h=0.8m, H=0.15m, T=1.436s, h/L=26.7% and H/L=5%; C1-C3)

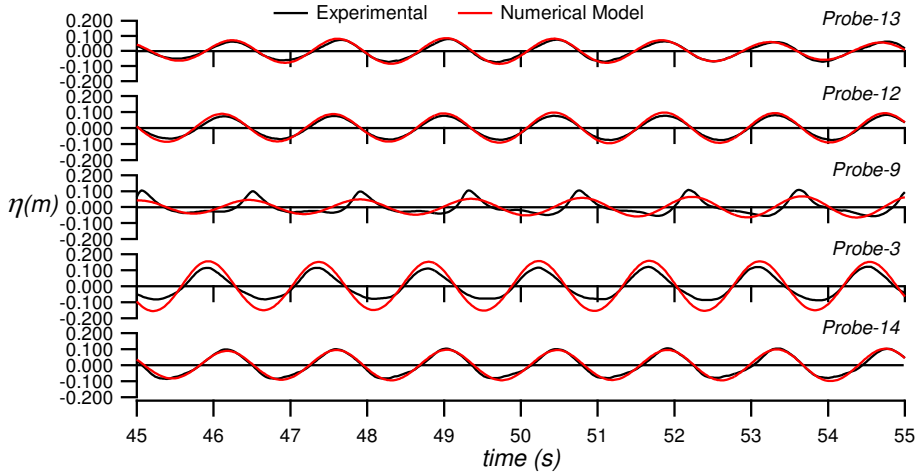

Fig. 8 Surface elevations at different probe locations in the presence of Columns 1-2-3-4 (Case3: h=0.8m, H=0.15m, T=1.436s, h/L=26.7% and H/L=5%; C1-C2-C3-C4)

Photo 1: Column 1-2-3-4 are shown in the Offshore Engineering Basin (OEB) of NRC

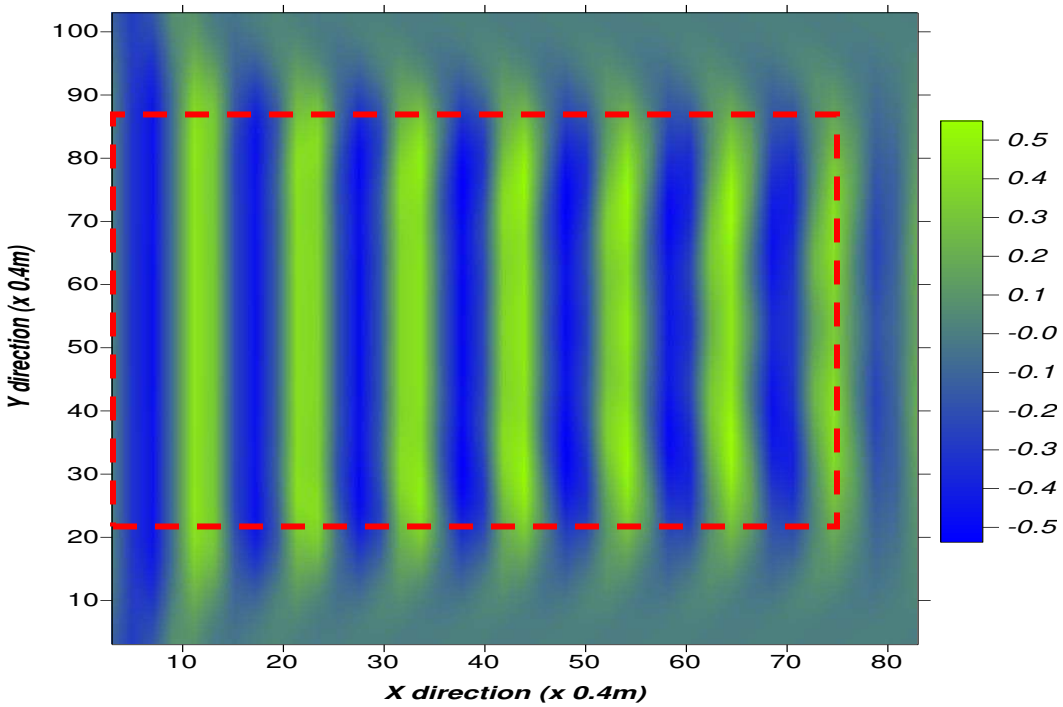

Fig. 9: Normalized wave heights on the flat bottom in the absence of columns (Case3: h=0.8m, H=0.20m, T=1.736s, h/L=0.2 and H/L=5%)

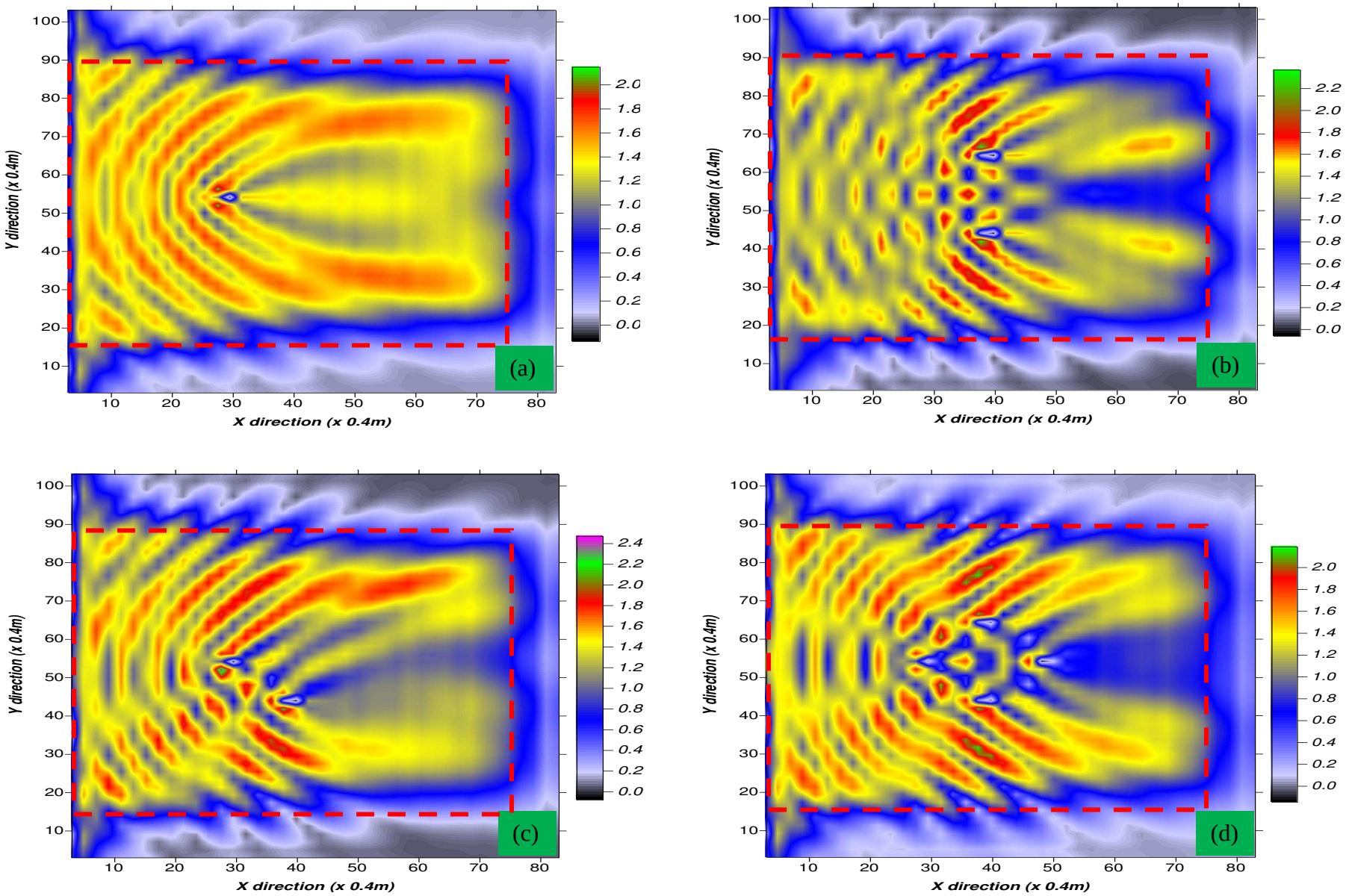

Fig. 10: (a) Normalized wave heights for column C3; (b) Normalized wave heights for column C1-2; (c) Normalized wave heights for column C1-3; (d) Normalized wave heights for column C1-2-3-4 (Case3: h=0.8m, H=0.20m, T=1.736s, h/L=0.2 and H/L=5%)